Kinetics Study of *Bungarus fasciatus* Venom Acetylcholinesterase Immobilised on a Langmuir–Blodgett Proteo-Glycolipidic Bilayer

Stéphanie Godoy,[a] Sébastien Violot,[b] Paul Boullanger,[c] Marie-Noëlle Bouchu,[c] Béatrice D. Leca-Bouvier,[a] Loïc J. Blum,[a] and Agnès P. Girard-Egrot*[a]

This study deals with the kinetics properties of an enzyme immobilised in a defined orientation in a biomimetic environment. For this purpose, acetylcholinesterase (AChE) was captured at the surface of a nanostructured proteo-glycolipidic Langmuir–Blodgett film through specific recognition by a noninhibitor monoclonal antibody (IgG) inserted in a neoglycolipid bilayer. Modelling of this molecular assembly provided a plausible interpretation of the functional orientation of the enzyme. The AChE activity being stable for several weeks, the enzyme kinetics were investigated, and fitted perfectly with heterogeneous biocatalytic behaviour representative of cellular enzymatic catalysis. The AChE–IgG–glycolipid nanostructure was directly interfaced with an efficient optical device. Such an association, leading to an intimate contact between the nanostructure and the biochemical signal transducer, gives direct access to the intrinsic AChE behaviour. This study thus demonstrates the potential for direct investigation of the kinetic behaviour of an immobilised enzyme on a lipid bilayer through an efficient transduction system.

It has been recognised for many years that numerous enzymes of living cells are localised on or within membranous structures.[1] Such an enzyme location implies the presence of a microenvironment around the protein molecules, thus modifying their apparent kinetic behaviour relative to that seen with soluble enzymes. This microenvironment, also named a diffusion layer, can be regarded as a quiescent area where metabolites diffuse. Cellular catalysis mainly operates through immobilised enzymes localised in unstirred compartments, so studies of enzyme behaviour in a homogenous environment are not sufficiently relevant to explain and understand enzymatic processes occurring in vivo. For this reason it appears essential to investigate enzyme behaviour in a heterogeneous phase, and to this end artificial enzyme membranes still remain interesting experimental tools for studing the interplay between mass-transfer phenomena and enzyme reactions under well-defined conditions.[2–4]

Enzyme immobilisation can be carried out on various synthetic supports with defined characteristics, and many studies with numerous polymeric membranes have been performed in order to investigate such heterogeneous enzymatic behaviour.[5–7] Some of this work, dealing with enzymes trapped on a collagen membrane, indicated enhancement of the apparent enzyme stability after protein immobilisation.[8–10] The long-lasting activity of the enzyme trapped in a solid matrix has recently been confirmed by using various immobilising matrices[11–13] and attributed either to a stabilisation effect of the embedding or to the beneficial influence of diffusional limitations. This microenvironment effect induced an increase in the substrate concentration (S) at which the rate of the heterogeneous enzymatic reaction was half the saturation rate. This particular substrate concentration, in some cases misleadingly termed apparent K_M, is named $S_{0.5}$ and has largely been interpreted by Engasser and Horvath,[14] or in our group,[15–18] in terms of substrate diffusion from the bulk solution towards the catalytic sites. One proposed method to reduce the diffusional effects on the enzyme activities measured in the bulk is through more efficient stirring of the reaction medium.[14] Another possibility is to lower the immobilised enzyme activity by, for example, reducing the amount of immobilised biocatalyst.

Langmuir–Blodgett (LB) technology allows lamellar lipidic stacks to be built by transferring a monomolecular film, formed at an air/water interface, onto a solid support, with accurate control of the thickness and of the molecular organisation. Based on the self-assembly properties of amphiphilic biomolecules, this technique offers the possibility of preparing ultrathin lipid layers suitable for enzyme immobilisation. Like biological bilayers, LB films appear to be good candidates for developing biomimetic models and investigating enzyme kinetics behaviour in biomimetic environments. In the first studies performed in our group to associate enzymes with lipidic

[a] *S. Godoy, Dr. B. D. Leca-Bouvier, Prof. L. J. Blum, Dr. A. P. Girard-Egrot*
Laboratoire de Génie Enzymatique et Biomoléculaire
EMB2 UMR 5013—CNRS/UCBL
Université Claude Bernard Lyon 1
43 Bvd du 11 novembre 1918, 69622 Villeurbanne Cedex (France)
Fax: (+33) 4-72-44-79-70
E-mail: agnes.egrot@univ-lyon1.fr

[b] *S. Violot*
Laboratoire de BioCristallographie
Institut de Biologie et Chimie des Protéines
UMR 5086—CNRS/UCBL, IFR 128 Biosciences Lyon–Gerland
7 passage du Vercors, 69367 Lyon Cedex 07 (France)

[c] *Dr. P. Boullanger, M.-N. Bouchu*
Laboratoire de Chimie Organique 2, UMR 5181—CNRS/UCBL
Université Claude Bernard Lyon 1
Ecole Supérieure de Chimie Physique Electronique de Lyon
43 Bvd du 11 novembre 1918, 69622 Villeurbanne Cedex (France)

 DOI: 10.1002/cbic.200400277

LB films, we were able to show clearly that an extremely low enzyme activity was effectively retained on LB surfaces.[19–21] The first investigation of the enzyme kinetic behaviour of choline oxidase, randomly adsorbed onto preformed lipidic LB films, revealed that the enzyme behaviour was not under substrate diffusional control, but under enzymatic control.

With the aim of accurately assessing the kinetics properties of an immobilised enzyme in a defined orientation, we had previously designed an organised proteo-lipidic LB nanostructure geared towards the sequestration of a hydrophilic enzyme at the surface of a neoglycolipid bilayer.[18] By inserting a noninhibitor monoclonal antibody (IgG) directed against the soluble acetylcholinesterase monomer (AChE), this structure enables the enzyme to be bound in a functional position at the surface of the lipidic matrix. Previous results have shown that the enzyme stability allows the direct measurement of the AChE activity over a long period of time.[18]

In this paper, modelling of the ternary biomimetic molecular assembly (AChE–IgG–glycolipid) has been achieved for the first time, providing insights into the molecular orientation of the AChE–IgG immune complex in the glycolipid bilayer. The stability of the ternary nanostructure as a function of the hydrocarbon chain length of the neoglycolipid molecule was then investigated in order to define experimental conditions giving access to the kinetic properties of the immobilised enzyme. Hence, a careful analysis of the biocatalytic behaviour of AChE bound onto the lipidic bilayer was performed. Finally, the AChE–IgG–glycolipidic molecular assembly was directly interfaced with an efficient optical device. Such an association, leading to intimate contact between the biomimetic nanostructure and the biochemical signal transducer, allows molecular recognition and signal transduction in a single device, as in the biological membrane.

Results and Discussion

AChE–IgG–GC11 nanostructure modelling

In our previous work devoted to the design of the ternary Langmuir–Blodgett nanostructure, we assumed that the functional position of the IgG in the glycolipid matrix could be attributed to the strong interactions between IgG and neoglycolipid molecules. Indeed, carbohydrate–carbohydrate interactions between the glycolipid headgroup and the glycans of the IgG molecule, and/or hydrophobic interactions between the glycolipid and the hydrophobic Fc fragment of the immunoglobulin, could be inferred at the molecular level. In order to check such a hypothesis, the more likely arrangement of the biomimetic nanostructure was tested by modelling the AChE–IgG–GC11 assembly (Figure 1). Modelling of each component (*Bungarus fasciatus* AChE, IgG and GC11) is described in the Experimental Section. The interaction surface between

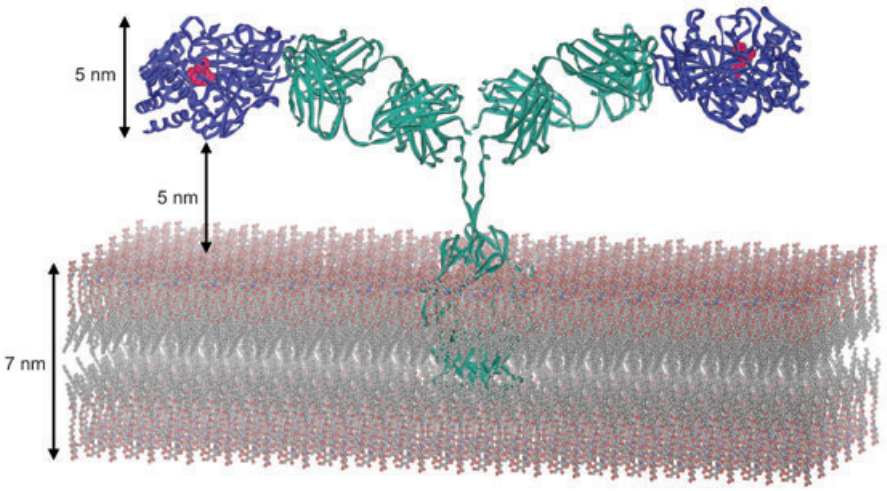

Figure 1. *Structural modelling of the functional Langmuir–Blodgett (LB) AChE–IgG–glycolipidic molecular assembly.*

AChE and IgG was then chosen by taking into account the glycosylation sites of AChE[22] (N289, N374, N484 and N564) in order to avoid steric hindrance between AChE glycans and the antigen-binding site of IgG defined by its variable loops CDR1–CDR3.[23] Thus, the mouth of the "active site gorge" is opposite to the enzyme–IgG interface and is accessible to solvent. Such an orientation should favour accessibility of the active site by the substrates and would be compatible with the noninhibitory properties of the designed antibodies.[22] The AChE–IgG complex was inserted in turn into the bilayer model. We assume that the IgG–Fc domain is anchored in one half of the lipidic membrane and lies on the hydrophobic moiety of the lower layer. In such a model, the *N*-linked oligosaccharides bound to the strictly conserved Asn127 of the IgG effectively interact with the lipidic polar head of the upper layer.[24] The polar head of the lower glycolipid monolayer cannot be disturbed by the insertion of the immune complex, and the active site of the enzyme is located at about 50 Å from the membrane surface. This modelling gives a plausible account for a suitable enzyme orientation at the surface of the lipidic bilayer.

The molecular structure model occupies a surface of 280×110 Å^2. With a solid support surface of 5.5 cm^2, the theoretical maximum number of deposited complexes is 1.78×10^{12}. In order to compare in silico and in vitro results, the number of complexes transferred onto the support was estimated. Taking into account the maximal enzyme activity retained in the nanostructure under saturating conditions and the acetylcholinesterase turnover number, 9.24×10^{11} AChE molecules are immobilised. If two AChE are bound per IgG, 4.62×10^{11} IgG–AChE complexes are correctly inserted, that is, 3.85 times lower than the maximum theoretical value. Such in vitro and in silico

results appear to be in good agreement, considering the space necessary for specific recognition between an antigen and an antibody.

Stability of the ternary structure as a function of the glycolipid chain length

The molecular assembly, and consequently the immobilised enzyme activity, must be stable over a long period of time in order to achieve an accurate biocatalytic study. With the aim of exploring the functional stability of the AChE–IgG–glycolipid LB film, two ternary structures were built from two glycolipid analogues bearing different hydrocarbon chains ("GC11", with 11 carbons, and "GC14", with 14 carbons in their chain lengths). In order to check their stability, AChE–IgG–glycolipid complexes were stored in a buffered solution (0.1 M phosphate buffer pH 7.4, 0.15 M NaCl, 1 mg mL^{-1} BSA), and the retained AChE activity was regularly measured by Ellman's colorimetric method,[24] over a period of about 80 days (Figure 2). First of

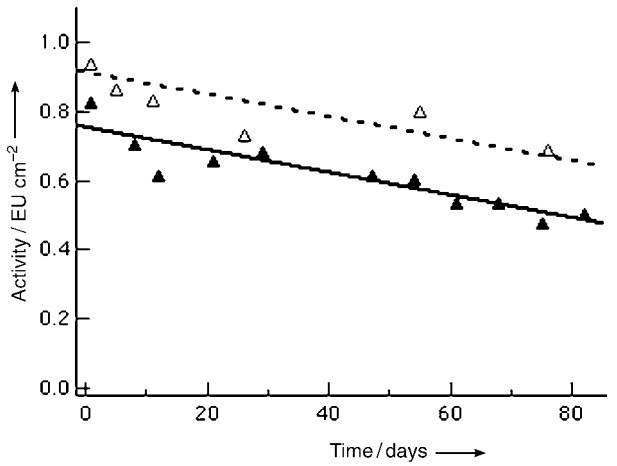

Figure 2. *Time-dependant enzyme activity observed after AChE immunoimmobilisation on mixed IgG–glycolipid bilayers formed from GC11 (full line) or GC14 (dashed line).*

all, it can be seen that the AChE–IgG–GC14 molecular assembly retains a higher activity than the AChE–IgG–GC11 structure. Furthermore, in both cases, the activity decreases only moderately over the investigated period of time: losses of 35% and 30% were observed for AChE–IgG–GC11 and AChE–IgG–GC14 ternary complexes, respectively. To the best of our knowledge, such a high stability has never before been reported for an immobilised enzyme on a bilayer obtained by the LB technique. For comparison, Puu and Ohlsson's group[26,27] reported a half-life of only 28 days for the activity of AChE immobilised by fusion of proteo-phospholipidic vesicles onto solid substrates. Additionally, it must be stressed that no enzyme desorption was observed in our experiments when the plate was removed from the enzyme substrate medium. The strong retention of AChE–IgG immune complexes on the glycolipid bilayer can be attributed to a combined effect of the specificity of IgG–AChE recognition and the strong proteo-lipidic interactions between IgG and neoglycolipid molecules, as shown by the molecular structure modelling. Finally, no determinant influence of the glycolipid hydrocarbon chain length on the molecular stability was observed.

Kinetic study of AChE immobilised on the lipidic matrix with a hydrocarbon chain length of $n = 11$

As previously shown,[14] the apparent enzymatic behaviour of an immobilised enzyme is clearly dependent on the enzyme activity retained on the support. To investigate the enzymatic kinetics of AChE immobilised on the lipidic bilayer, five IgG–glycolipid molecular assemblies retaining five different amounts of the enzyme were prepared. For this purpose, supports coated with IgG–GC11 bilayers were immersed into AChE solutions at different concentrations, allowing different enzyme activities to be retained (1.3, 0.8, 0.5, 0.3 and 0.07 EU cm^{-2}). By taking the surface occupied by an AChE–IgG complex in the orientated position[28] ($\approx$60 nm^2) and the turnover number of the enzyme into account, it could be estimated that the percentages of the monolayer area occupied by active IgG–AChE complexes were 5, 3, 1.8, 1 and 0.3, respectively, for each support.

The velocities of the reaction catalysed by the immobilised AChE on each support were measured by varying the acetylthiocholine concentrations. The normalised rates of reaction (V/V_m) as a function of the acetylthiocholine concentration were compared with those catalysed by the soluble enzyme (direct plots, Figure 3A). It should be mentioned that soluble AChE is also inhibited at high substrate concentrations, as well as in the immobilised forms. The soluble AChE displays kinetics (curve a) and a K_M value (0.04 mM) in agreement with the results reported in the literature.[22,29] The immobilised enzyme exhibiting lower activity behaves quite similarly to the soluble form (curve b). For higher amounts of immobilised enzyme (curves c to f), it can be seen that the kinetic curves are shifted towards higher acetylthiocholine concentrations, showing the presence of external diffusional resistances of substrate from the bulk to the enzyme microenvironment. Eadie–Hofstee-type representation can be used to illustrate the effect of the diffusional resistances on the enzyme kinetic behaviour.[30,31] In our case, this representation clearly indicates that the increase in the diffusional resistance is directly correlated to the retained enzyme activity. For the support retaining a lower AChE activity (0.072 EU cm^{-2}, Figure 3B, curve b), the external transport limitations are negligible and the plot is quite similar to that of soluble AChE. For higher retained AChE activity (curve f), on the other hand, the external transport limitations become predominant.

These observations can be directly correlated to the $S_{0.5}$ values determined for each support by the Hanes graphical representation ([ATChI]/V vs. [ATChI]) (Table 1). It appears that $S_{0.5}$ values differ from that of the soluble enzyme: $S_{0.5} > K_M$. The higher the immobilised enzyme activity, the higher the $S_{0.5}$ value, indicating an increase in the diffusional resistance effects. These experimental results can be interpreted by the

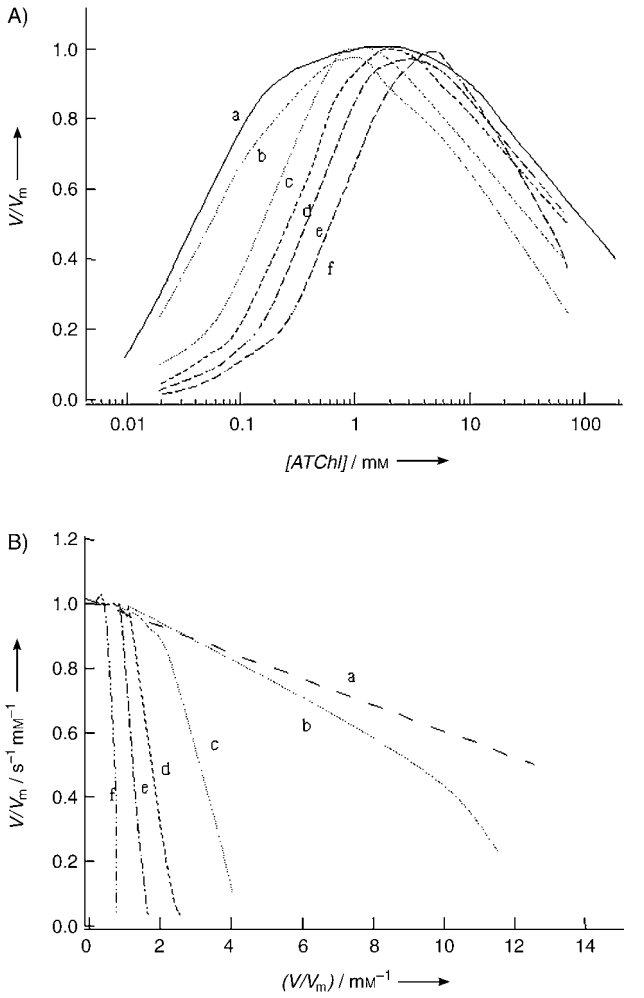

Figure 3. *Enzymatic kinetics of AChE immobilised on the IgG–GC11 molecular assembly. A) direct plot, and B) Eadie–Hofstee plot. a) AChE in solution, together with immobilised AChE at: b) 0.072 EU cm^{-2}, c) 0.29 EU cm^{-2}, d) 0.48 EU cm^{-2}, e) 0.78 EU cm^{-2}, and f) 1.33 EU cm^{-2}.*

Table 1. *$S_{0.5}$ values of AChE immobilised on IgG–GC11 or IgG–GC14 nanostructures.*

GC11		GC14	
Immobilised enzyme activity [EU cm^{-2}]	$S_{0.5}$ [mM]	Immobilised enzyme activity [EU cm^{-2}]	$S_{0.5}$ [mM]
0.07	0.08	0.04	0.09
0.3	0.3	0.16	0.3
0.5	0.6	0.3	0.6
0.8	0.9	0.7	0.9
1.3	1	–	–

postulate that not all the reacting species can reach the immobilised enzyme molecules. It is to be expected that, for a high amount of immobilised enzymes, the enzyme kinetics should be controlled by the mass transfer process.[14] In contrast, the kinetic behaviour of a low-amount immobilised enzyme stays under kinetics control, due to a limited effect of substrate diffusional resistances.

Kinetics of AChE immobilised on the lipidic matrix with a hydrocarbon chain length of $n = 14$

A similar study was carried out for AChE immobilised on a lipidic bilayer made of the glycolipid presenting a 14-carbon atom chain length. For this purpose, four IgG–GC14 molecular assemblies retaining different enzyme activities were designed. As described above, the IgG–glycolipid-coated supports were immersed in four different AChE concentrations, thus ensuring enzyme activities per plate of 0.7, 0.3, 0.16 and 0.04 EU cm^{-2}. The estimated percentages of the deposited monolayer area occupied by active IgG–AChE complexes were 2.6, 1.2, 0.6 and 0.14, respectively, for each support. Direct (Figure 4A) and Eadie–Hofstee (Figure 4B) plots were drawn for each set of experiments. It can be seen that the immobilised AChE behaves similarly whether the lipidic bilayer is composed either of GC14 or of GC11. Table 1 shows that the $S_{0.5}$ values obtained with GC14 are always higher than K_M, as previously underlined for GC11. For both glycolipidic matrices, $S_{0.5}$ increases with the

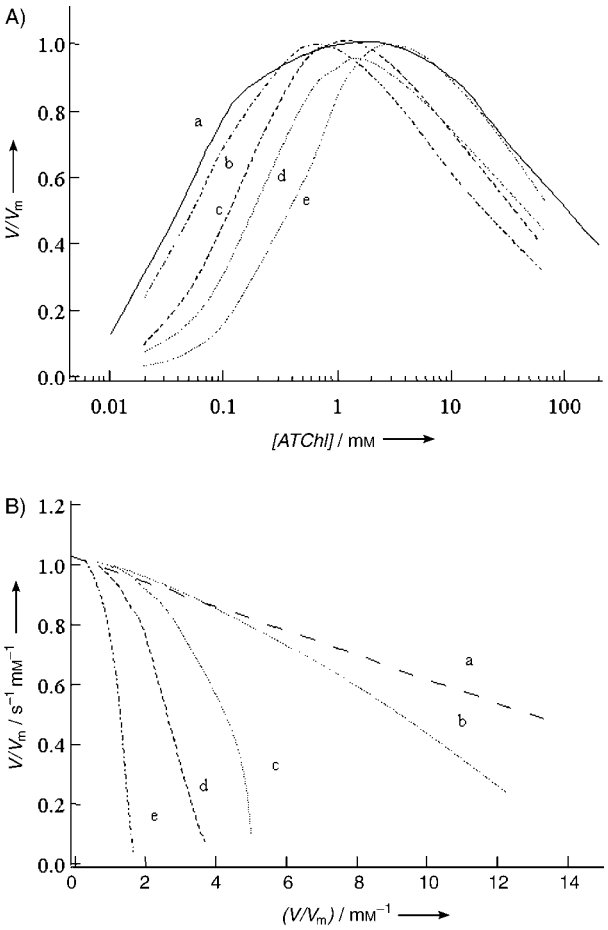

Figure 4. *Enzymatic kinetics of AChE immobilised on the IgG–GC14 molecular assembly. A) direct plot and B) Eadie–Hofstee plot. a) AChE in solution, together with immobilised AChE at: b) 0.036 EU cm^{-2}, c) 0.16 EU cm^{-2}, d) 0.313 EU cm^{-2}, and e) 0.704 EU cm^{-2}.*

immobilised enzyme activity. This effect clearly indicates the occurrence of diffusional limitations, as previously shown for immobilised enzymes on synthetic membranes.[9,15] For high enzyme activity the $S_{0.5}$ value remains close to 1 mM, whereas the intrinsic K_M value is 0.04 mM. It must be stressed that, for a precise $S_{0.5}$ value, the retained enzyme activity is always higher for GC11 than for GC14. For instance, an $S_{0.5}$ value equal to 0.3 mM is obtained with an AChE activity of 0.3 EU cm^{-2} on the GC11 nanostructure, rather than 0.16 EU cm^{-2} for GC14. These results demonstrate that the external transport limitations occurring for GC11 are less pronounced than for GC14. This can be correlated to a difference in the diffusional layer thickness. In fact, some IgG moieties have been transferred onto the first deposited layer, so the immobilised AChE retained by the IgG could be slightly buried in the bilayer. For the internally located AChE, the enzymatic substrate and product have to diffuse to reach the active site gorge. As the difference between GC11 and GC14 only concerns the carbon chain length, more internal diffusional resistances correlated to a thicker bilayer occur in the case of GC14. It must be underlined that the model shown in Figure 1 is the more probable one.

Potential of the biomimetic molecular assembly to assist study of the intrinsic biocatalytic behaviour of an immobilised enzyme

The enzymatic behaviour of AChE immobilised on the lipidic bilayer is typical of heterogeneous biocatalysis, widely investigated with micrometric polymeric membranes.[8,9,15,32,33] Usually, biocatalytic behaviour studies of immobilised enzymes are performed with the enzymes either directly immobilised on solid (graphite) surfaces[12] or entrapped in polymeric membranes[14,15,34] and placed in a reaction medium stirred at different speeds. Measurement of the reaction rates can thus be performed under defined hydrodynamic conditions, allowing control over the external diffusional resistances of the substrate from the bulk solution to the enzyme microenvironment or of the product from the microenvironment to the bulk phase. In our case, controlled hydrodynamic conditions induced by stirring variation cannot be applied because the molecular assembly needs to be cautiously handled. However, the ability to control the amount of enzyme retained on the LB structure, through control of saturation of IgG recognition sites, appears to be a good alternative for investigating immobilised enzyme biocatalytic behaviour under modulated diffusional resistance conditions. In particular, the retention of an extremely low enzyme activity (below 0.072 EU cm^{-2}), giving virtually the same enzymatic behaviour as the soluble enzyme, offers the potential for direct access to the intrinsic enzyme behaviour. The proteo-glycolipidic LB nanostructure, then, appears to be an efficient biomimetic model for study of immobilised enzyme behaviour in a lipidic bilayer under low-stirring conditions, as in natural environments.

Association of a Langmuir–Blodgett nanostructure with an electrochemiluminescent device.

The enzymatic kinetics analysis described above was performed with a biomimetic structure transferred onto an inert support (functional area of 5.5 cm^2), with the use of Ellman's classical colorimetric method for acetylcholinesterase activity detection.[25] The down-scaling of the working area is an important point that must be considered with a view to achieving analysis at the molecular level. Furthermore, direct signal transduction of the molecular recognition events appears more relevant from a biomimetic point of view. With the double aim of miniaturising and directly interfacing the biomimetic sensing layer with an efficient signal transducer, the AChE–IgG–glycolipid complex has been associated with an optical device previously developed in our group for choline detection[35] (Figure 5). Briefly, choline oxidase (ChOD) is entrapped in a photopolymer on a screen-printed electrode maintained at a potential allowing oxidation of luminol present in solution. The ternary AChE–IgG–GC11 structure was directly transferred onto the working electrode (detection area of 0.18 cm^2). Choline was thus produced from acetylcholine upon AChE reaction and was detected by luminol electrochemiluminescence (ECL) after its oxidation into the corresponding betaine and hydrogen peroxide by choline oxidase. Figure 6 shows the ECL response recorded after injection of acetylcholine. A linear response is obtained from 0.4 μM to about 40 μM of acetylcholine. Hence, the miniaturisation of the analysed area has been successful, and the direct interfacing with a functional device has revealed the potential for detection of very low acetylcholine concentrations (detection limit of 0.4 μM). Beyond the 40 μM value corresponding to the K_M of AChE, the device does not display a linear response. This behaviour reveals that the immobilised AChE is in saturating substrate conditions. Furthermore, the immobilised enzyme preparation is not limited by diffusional resistances. Indeed, these are usually able to extent the linear sensor response at substrate concentrations higher than the enzyme K_M value. The normalised optical signal obtained by ECL detection, expressed as I/I_m (where I corresponds to the luminescent intensity and I_m the maximum) versus the acetylcholine (ACh) concentration (curve a,

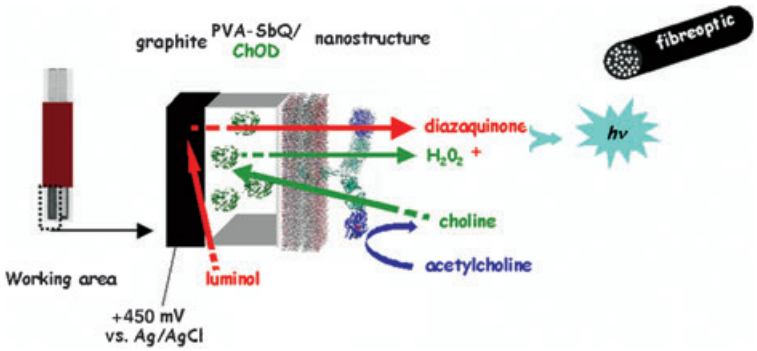

Figure 5. *Langmuir–Blodgett nanostructure deposited onto a screen-printed electrode.*

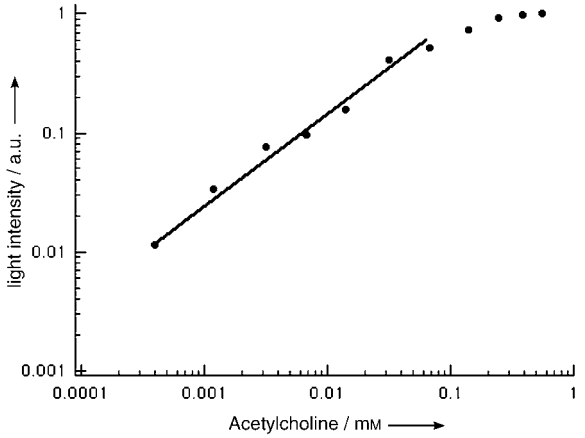

Figure 6. *ECL signal versus acetylcholine concentration, obtained with the AChE–IgG–GC11 biodevice.*

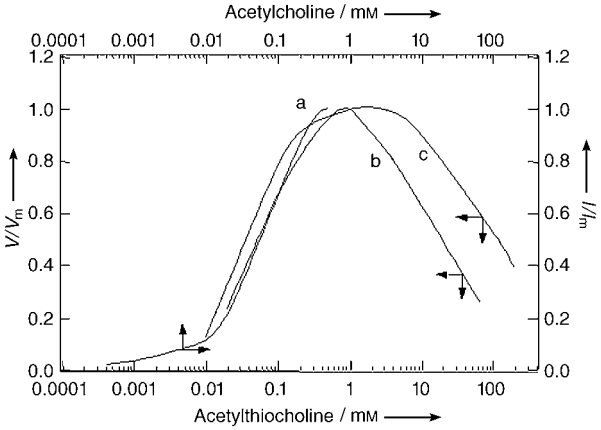

Figure 7. *Enzymatic kinetics of AChE immobilised on the IgG–GC11 molecular assembly. a) Associated with the ECL device. b) Investigated by Ellman's method at low substrate diffusional resistances. c) Enzymatic kinetics of the soluble AChE.*

Figure 7), was compared both with the normalised activity previously measured by Ellman's method at low substrate diffusional constraints (curve b, Figure 7) and with that obtained by Frobert et al.[29] for the soluble enzyme (curve c, Figure 7). Evidently, the ECL optical response (curve a) virtually superimposes with the enzymatic kinetics of the soluble AChE (curve c); this indicates that the ECL sensor response reflects the enzyme kinetics of the AChE immobilised on the lipidic structure. Therefore, the intimate contact of the molecular assembly with an optical device leads to direct investigation of the enzyme kinetics. The potential for direct access to the enzymatic behaviour of AChE immobilised on the biomimetic nanostructure through efficient transduction of the biochemical signal, mimicking that of biological membranes, has been demonstrated. To the best of our knowledge, no such association between a LB structure and an ECL device has ever previously been reported. This new kind of LB-bio-optoelectronic device thus appears to be a powerful tool for investigation of immobilised enzyme kinetics in a biomimetic environment and for approaching fine microanalysis at the molecular level.

Conclusion

In order to perform accurate heterogeneous biocatalysis in a biomimetic situation, a polyvalent nanostructure based on the specific recognition of a noninhibitor antibody has been designed.[18] In this work, modelling of this molecular assembly has confirmed the molecular arrangement proposed on the basis of experimental data.[18] Indeed, the functional orientation of AChE–IgG immune complexes in the bilayer structure in silico is plausible with respect to the steric hindrance induced by the immobilization of several complexes. The main characteristic of this molecular association is to maintain a hydrophilic enzyme close to the lipidic membrane in an orientated position.

This organised biomimetic structure has been demonstrated to be adaptable for biocatalysis investigations of an immobilised enzyme in a lipidic environment. To the best of our knowledge, only a few biocatalytic studies using Langmuir–Blodgett films have been published to date.[21,36] The typical enzymatic behaviour of the ternary complex (AChE–IgG–glycolipid) clearly demonstrates the potential usefulness of such a functional molecular assembly for accurate biocatalysis studies. The apparent AChE activity measured by Ellman's method evidently results from diffusional constraints. By using two glycolipids varying in their carbon chain lengths, a difference has been noticed in terms of diffusional limitations and is thought to be linked to the substrate accessibility towards the enzyme located in the lipidic layer.

Finally, the intimate association of these membranes with a performant ECL detection system has indicated the potential for direct measurement of the intrinsic AChE activity without any diffusional resistances. It is therefore possible to approach molecular recognition and signal transduction events in a single device. This is very promising for development of biomimetic nanosensors and minute investigations of biological processes at the molecular level. All IgG structures being similar, this model could be extendable to antibodies of various specificities, thus affording a device of general interest.

Experimental Section

Materials: The synthetic glycolipids used as the lipidic matrix differ in their hydrocarbon chain lengths (GC11, $n=11$, GC14, $n=14$) (Scheme 1).

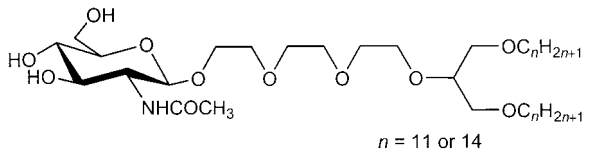

Scheme 1. *Structures of the synthetic glycolipids (GC11,* n = *11, GC14,* n = *14).*

GC11 (10-undecyloxymethyl-3,6,9,12-tetraoxatricosyl 2-acetamido-2-deoxy-β-D-glucopyranoside) was synthesised as previously reported.[37] GC14 (10-tetradecyloxymethyl-3,6,9,12-tetraoxahexacosyl 2-acetamido-2-deoxy-β-D-glucopyranoside) was prepared as al-

ready described for the analogues with C_{11} and C_{16} dialkyl chains.[37] Thus, epichlorohydrin was condensed with tetradecanol in THF and HMPA in the presence of NaH to afford 1,3-bis(tetradecyloxy)propan-2-ol in 19% yield. The ^{1}H and ^{13}C NMR spectra were identical to those already reported for the diC_{16} analogue (±0.2 ppm). Elemental analysis calcd (%) for $C_{31}H_{64}O_3$ (M_W 484.84): C 76.80, H 13.31; found C 76.69, H 13.40. This compound was condensed with triethyleneglycol dichloride under phase-transfer conditions (NaOH, Bu_4NHSO_4) to afford 1-chloro-10-tetradecyloxymethyl-3,6,9,12-tetraoxahexacosane in 38% yield. The chloro terminus was then hydrolysed in two steps [1) HCOONa, Bu_4NBr. 2) NaOH, H_2O] to afford 10-tetradecyloxymethyl-3,6,9,12-tetraoxahexacosan-1-ol in 84% yield. The ^{1}H and ^{13}C NMR spectra were identical to those already reported for the diC_{16} analogue (±0.2 ppm). Elemental analysis calcd (%) for $C_{37}H_{76}O_6$ (M_W 617.00): C 72.03, H 12.42; found C 71.87, H 12.19. This derivative was condensed with 1,3,4,6-tetra-*O*-acetyl-2-allyloxycarbonylamino-2-deoxy-β-D-glucopyranose[38] in CH_2Cl_2, in the presence of trimethylsilyl triflate, to afford the expected β-glucoside in 72% yield. This was finally deprotected in aqueous NaOH (4 N) and re-*N*-acetylated to afford 10-tetradecyloxymethyl-3,6,9,12-tetraoxahexacosyl 2-acetamido-2-deoxy-β-D-glucopyranoside in 78% yield. The ^{1}H and ^{13}C NMR spectra were identical to those already reported for the diC_{16} analogue (±0.2 ppm). Elemental analysis calcd (%) for $C_{45}H_{89}NO_{11}$ (M_W 820.19): C 65.90, H 10.94, N 1.71; found C 65.63, H 11.01, N 1.63.

Phosphate buffer subphases and other buffer solutions were prepared with ultrapure water (resistivity = 18.2 MΩ cm obtained from a milli-Q four-cartridge purification system (Millipore, France). Rectangular calcium fluoride plates (35×9.5×2 mm) purchased from Sorem (France) were used as transfer substrates after a cleaning procedure already described.[39] The immunoglobulin (monoclonal antibody directed against AChE of *Bungarus fasciatus* venom), generously supplied by Dr. Grassi (SPI, CEA Saclay, Gif-sur-Yvette, France), was purified on a Protein A HyperD F chromatography system (BioSepra, France) as reported elsewhere.[40] The nonamphiphilic water-soluble monomer of *Bungarus fasciatus* AChE was a generous gift from Dr. Bon (Institut Pasteur de Paris, Unités des Venins, France). *S*-Acetylthiocholine iodide (ATChI), 5,5′-dithiobis(2-nitrobenzoic acid) (DTNB, Ellman's reagent), luminol (3-aminophthalhydrazide), choline, acetylcholine and IgG-free Bovine Serum Albumin (BSA) were purchased from Sigma–Aldrich Chimie (St Quentin Fallavier, France). Poly(vinyl alcohol) bearing styrylpyridinium groups (PVA-SbQ), purchased from Tokyo Gosei Kogyo, Chiba, Japan, presents the following characteristics: polymerisation degree 2300, saponification degree 88, SbQ content 1.06%, solid content 11.10%, pH 6.2.

Proteo-glycolipidic nanostructure: The IgG–glycolipid nanostructure was built with a combination of vesicle spreading and Langmuir–Blodgett techniques.[18] Mechanical dispersion was used to prepare glycolipid and proteo-glycolipidic vesicles at room temperature by the previously described procedure.[40] Briefly, glycolipid vesicles and IgG–glycolipid vesicles were prepared by dispersion of a dry glycolipid film (2.5 mg) either in phosphate buffer (10 mM, pH 7.4, 250 μL), or in the purified antibody solution (3.5–4 mg mL^{-1}, 250 μL), respectively. The final glycolipid concentration and protein/lipid molar ratio were 10 mg mL^{-1} and 1:550, respectively. The vesicle suspensions were used directly for the spreading procedure and could be stored without apparent modification of their spreading kinetics at 4 °C over a one week period for GC11, and at 30 °C for one day for GC14. The interfacial films were prepared with a computerised KSV 3000 Langmuir–Blodgett trough (KSV Instrument Ltd., Finland) working in a symmetrical compression mode. The surface pressure was measured with a platinum Wilhelmy plate with an accuracy of ±0.05 mN m^{-1}. The interfacial films were formed onto a five-fold concentrated phosphate-buffered saline (PBS) solution (10 mM, pH 7.4, used as the subphase) and thermostated at 20 °C ± 0.5 °C for GC11 and 25 °C ± 0.5 °C for GC14. The transfer of the interfacial film onto calcium fluoride was performed by a vertical Langmuir–Blodgett film deposition procedure. In order to avoid any protein adsorption on the substrate,[41] this was rapidly immersed in the aqueous subphase after the 35 min lag-time following the spreading procedure. The monolayer was then compressed (15 cm^2 min^{-1}), until the defined transfer surface pressures for GC11 (30 mN m^{-1}) or GC14 (29 mN m^{-1}) were reached. Two monolayers, the first one at the upstroke and the second one at the downstroke, were transferred onto calcium fluoride substrates pre-coated with four behenic acid layers, with a rate of 5 mm min^{-1}. This pre-coating, produced from a monolayer of behenic acid spread onto a NaCl (10^{-2} M), $MnCl_2$ (10^{-4} M) subphase,[42] was shown to be essential for the transfer of a glycolipid bilayer with the hydrophilic headgroups pointing to the surface.[43,44] In order to avoid respreading of the second transferred layer during the interfacial crossing, the plate had to be withdrawn from the aqueous subphase through the compressed monolayer, as recommended elsewhere.[45]

AChE immobilisation on the proteo-glycolipidic Langmuir–Blodgett film: An adapted procedure to immobilise AChE was developed. The plate coated with the proteo-lipidic layers was handled in a horizontal position in order to avoid any back transfer of the IgG–glycolipid film on crossing a liquid interface.[18] The cell was then carefully filled with AChE solution (0.1 M phosphate buffer, pH 7.4, 0.15 M NaCl, 1 mg mL^{-1} BSA) until the plate was completely immersed, and immunoassociation was left to complete for 18 h at 4 °C with gentle magnetic stirring. The plates were then washed twice, for 30 min, with the same buffer.

Modelling of AChE–IgG–GC11: The components of the ternary complex were modelled as follows. A blast search[46] for the complete sequence of *Bungarus fasciatus* AChE (Figure 8)[47] was performed against the Protein Data Bank[48] in order to detect homologous proteins of known structures. A maximum sequence identity of 66% on 542 residues was obtained for *Torpedo californica* venom acetylcholinesterase, determined by X-ray crystallography at 1.8 Å resolution (PDB code 1EA5). Residue substitution was performed by use of the CALPHA program.[49] The resulting model was energy-minimised with the aid of the CNS program by a conjugate gradient method.[50] Padlan's atomic structure of human antibody IgG1[51] was used for the immunoglobulin model. Finally, the bilayer model was built from 960 molecules of 10-undecyloxymethyl-3,6,9,12-tetraoxatricosyl 2-acetamido-2-deoxy-β-D-glucopyranoside (GC11), arranged in a rectangular patch of 280×110 Å^2. GC11 molecules were generated by use of the ISIS/Draw 2.3 program from MDL Information systems and positioned on a graphics station with the aid of the Turbo-Frodo program[52] to form a bilayer model. The resulting model was minimised with the CNS program.[50]

Enzyme activity measurements: The activity of immobilised AChE was determined by Ellman's colorimetric method[25] with acetylthiocholine (ATChI) as the enzyme substrate, in the presence of DTNB (0.25 mM) in a phosphate buffer (0.01 M, pH 7.4) according to the following sequential reactions:

$$\text{acetylthiocholine} \xrightarrow{\text{AChE}} \text{acetate} + \text{thiocholine} \quad (1)$$

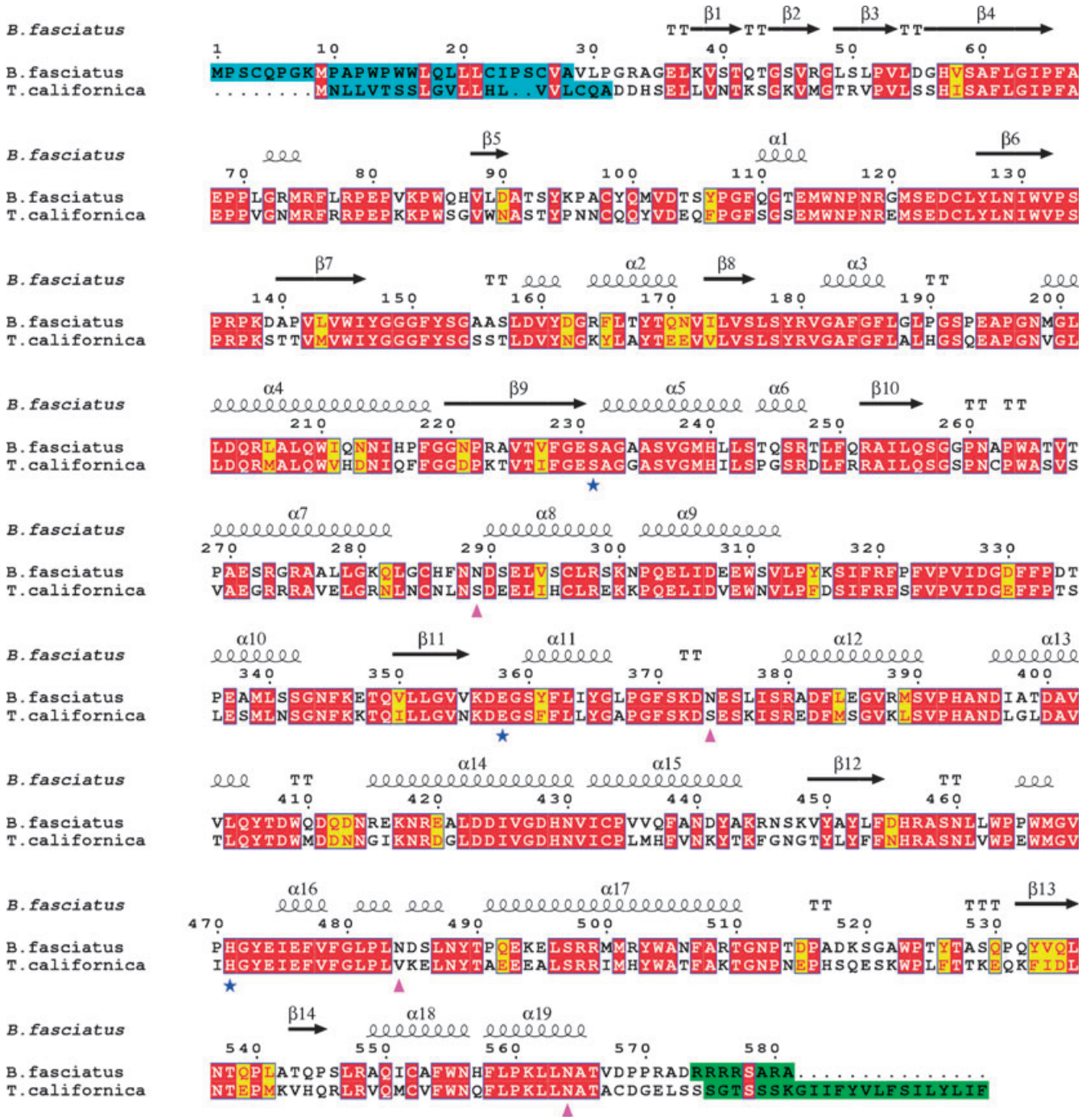

Figure 8. *Sequence comparison of AChE from* B. fasciatus *and AChE from* T. californica*, presented by the program ESPript.*[47] *Catalytic residues are indicated (blue stars), as are potentially glycosylated residues (pink triangles). The peptide signal and the propeptide, cleaved in the mature enzymes, are highlighted in blue and green, respectively.*

thiocholine + DTNB → 2-nitrobenzoyl-5-mercaptothiocholine + TNB (2)

The cell containing the plate previously coated with AChE was carefully filled with a defined volume of the enzyme substrate mixture until complete immersion of the plate. The hydrolysis of the enzyme substrate was monitored at 25 °C over two minutes through the production of a yellow compound (TNB) detected at 412 nm. The spontaneous hydrolysis of the substrate in the absence of the enzyme was also determined and routinely subtracted. The AChE activity retained on the solid plate was expressed in Ellman units per cm^2 (EU cm^{-2}). The non-specific adsorption of AChE onto glycolipid monolayers was also determined in the same way from layers of glycolipids transferred without antibody. Whatever the glycolipid matrix used, no non-specific adsorption could be detected.

Kinetic studies were performed for several acetylthiocholine concentrations both for soluble and for immobilised forms of AChE. For the assays with the soluble form, the reaction was directly initiated in a 25 °C thermostated cell by injection of enzyme (5.33 ng)

into the substrate reaction mixture. The number of experimental data points was about 10.

Electrochemiluminescent detection of the activity of immobilised AChE: The experimental ECL system, previously designed in our group, has been described elsewhere,[35] while Figure 5 depicts a schematic representation of the ECL system used. Briefly, it consists of a screen-printed electrode (4×0.6 cm) with a working electrode area of 0.18 cm^2 connected to a potentiostat (PRGE, Tacussel-Radiometer, Villeurbanne, France) and placed at 25 °C in a glass cuvette protected from ambient light. The cuvette was filled with stirring with veronal/HCl (30 mM, pH 9) containing luminol (50 μM, 2.5 mL). One end of a liquid core optical fibre (L.O.T. Oriel, Courtaboeuf, France) (core diameter 5 mm, overall diameter 7 mm) was positioned facing this electrode, with the other end connected to the photomultiplier tube of a luminometer (Biolumat, Berthold, Pforzheim, Germany). The screen-printed electrodes were produced in the Centre de Phytopharmacie (Perpignan, France) as two-electrode systems: a graphite working electrode and a printed Ag/AgCl reference electrode. The screen-printed electrodes were directly coated with an enzymatic film obtained by entrapping ChOD in a photopolymerised poly(vinyl alcohol) bearing styrylpyridinium groups (PVA-SbQ) by the procedure originally applied for enzyme immobilisation on a platinum macroelectrode.[53] The AChE–IgG–GC11 molecular assembly was directly interfaced onto the entrapped ChOD polymeric membrane by the following procedure. The working electrode was used as a Langmuir–Blodgett substrate, and the IgG–GC11 Langmuir monolayer was transferred at a surface pressure of 30 $mN\,m^{-1}$ by the same procedure as described above. After deposition, the IgG–GC11 electrode was immersed in an AChE enzymatic solution (34 $EU\,mL^{-1}$). The immunoassociation was performed over two hours at 4 °C with stirring. After immunoassociation, the electrode was rinsed twice for 20 min at 4 °C with stirring. After one night of storage at 4 °C, electrochemiluminescence measurements (in arbitrary units (au)) were performed on a graphic recorder (Servotrace, Sefram, Saint-Etienne, France). The potential application (+450 mV vs. Ag/AgCl) allows luminol oxidation on the working electrode. After stabilisation of the luminescent background signal, the ECL reaction was initiated by injection of either choline or acetylcholine into the buffer-filled cell. Upon AChE reaction, acetylcholine gives rise to choline, this then leading to H_2O_2 reacting with the oxidised luminol (diazoquinone), thus producing light. The sequential reactions for the electrochemiluminescent detection of acetylcholine are as follows:

$$\text{acetylcholine} + H_2O \xrightarrow{\text{AChE}} \text{acetate} + \text{choline} \quad (3)$$

$$\text{choline} + H_2O + 2\,O_2 \xrightarrow{\text{ChOD}} \text{betaine} + 2\,H_2O_2 \quad (4)$$

$$\text{luminol} + 2\,H_2O_2 \xrightarrow[+0.45\,V\ vs.\ Ag/AgCl]{\text{graphite}} \text{3-aminophthalate} + N_2 + 3\,H_2O + h\nu\ (\lambda_{max} = 425\,nm) \quad (5)$$

A steady-state light signal was reached after about 2 min. Different control experiments were performed to check that the ChOD loading was not limiting for AChE activity detection (data not shown).

Abbreviations

AChE: Acetylcholinesterase. ATChI: *S*-Acetylthiocholine iodide. ChOD: Choline oxidase. DTNB: 5,5′-Dithiobis (2-nitrobenzoic acid). ECL: Electrochemiluminescence. EU: Ellman's unit. GC11: Glycolipid with hydrocarbon chain lengths of 11. GC14: Glycolipid with hydrocarbon chain lengths of 14. IgG: Immunoglobulin G. K_M: Michaelis constant. LB: Langmuir—Blodgett. TNB: 5-Thio-2-nitrobenzoate. *S*: Substrate concentration. $S_{0.5}$: Substrate concentration at which the rate of the heterogeneous enzymatic reaction is half of the saturation rate. *V*: Enzymatic reaction rate. V_m: Maximum enzymatic reaction rate.

Acknowledgements

Thanks are due to Dr. J. Grassi (CEA, Saclay, France) for his generous gift of the ascitic fluid and to Dr. C. Bon (Institut Pasteur, Paris, France) for his generous gift of the acetylcholinesterase extracted from Bungarus fasciatus *venom, together with their interest in this work. Thanks to the laboratoire de BioCristallographie, directed by Dr. R. Haser, and especially to Dr. X. Robert and Dr. P. Gouet for their helpful discussion on the modelling.*

Keywords: heterogeneous catalysis · immobilized enzymes · Langmuir–Blodgett films · molecular modeling · protein orientation · signal transduction

[1] G. R. Welch, *Prog. Biophys. Mol. Biol.* **1977**, *32*, 103 – 191.
[2] B. Bunow, S. R. Caplan, *Biophys. J.* **1984**, *45*, 1065 – 1071.
[3] B. Maïsterrena, L. J. Blum, G. Bardeletti, P. R. Coulet, *Biochem. J.* **1986**, *235*, 693 – 698.
[4] J. C. Vincent, S. Alexandre, M. Thellier, *Arch. Biochem. Biophys.* **1988**, *261*, 405 – 408.
[5] P. R. Coulet, G. Bardeletti, F. Séchaud in *Bioinstrumentation and Biosensors*, (Ed.: D. L. Wise), Marcel Dekker, Inc., New York, Basel, Hong Kong, **1991**.
[6] C. H. Assolant-Vinet, P. R. Coulet, *Anal. Lett.* **1986**, *19*, 875 – 885.
[7] P. R. Coulet, J. H. Julliard, D. C. Gautheron, *Biotechnol. Bioeng.* **1974**, *16*, 1055 – 1068.
[8] J.- M. Engasser, P. R. Coulet, *Biochim. Biophys. Acta* **1977**, *485*, 29 – 36.
[9] J.- M. Engasser, P. R. Coulet, D. C. Gautheron, *J. Biol. Chem.* **1977**, *252*, 7919 – 7922.
[10] P. R. Coulet, D. C. Gautheron, *J. Chromatogr.* **1981**, *215*, 65 – 72.
[11] R. Gaffar, S. Kermasha, B. Bisakowski, *J. Biotechnol.* **1999**, *75*, 45 – 55.
[12] Q. Z. K. Zhou, X. D. Chen, *J. Food Eng.* **2001**, *48*, 69 – 74.
[13] Q. Z. K. Zhou, X. D. Chen, *Biochem. Eng. J.* **2001**, *4*, 33 – 40.
[14] J.-M. Engasser, C. Horvath in *Applied Biochemistry and Bioengineering* (Eds.: L. B. J. Wingard, E. Katchalski-Katzir, L. Goldstein), Academic Press, New York, **1976**, pp. 127 – 220.
[15] L. J. Blum, P. R. Coulet, *Biotechnol. Bioeng.* **1986**, *28*, 1154 – 1158.
[16] G. Bardeletti, B. Maïsterrena, P. R. Coulet, *Enzyme Microb. Technol.* **1986**, *8*, 365 – 369.
[17] A. P. Girard, B. Merchie, B. Maïsterrena, *Biochem. J.* **1991**, *274*, 819 – 824.
[18] S. Godoy, J.-P. Chauvet, P. Boullanger, L. J. Blum, A. P. Girard-Egrot, *Langmuir* **2003**, *19*, 5448 – 5456.
[19] L. Marron-Brignone, R. M. Morélis, L. J. Blum, P. R. Coulet, *Thin Solid Films* **1996**, *284–285*, 784 – 788.
[20] A. P. Girard-Egrot, R. M. Morélis, P. R. Coulet, *Thin Solid Films* **1997**, *292*, 282 – 289.
[21] A. P. Girard-Egrot, R. M. Morelis, P. R. Coulet, *Bioelectrochem. Bioenerg.* **1998**, *46*, 39 – 44.
[22] X. Cousin, C. Créminon, J. Grassi, K. Méflah, G. Cornu, B. Saliou, S. Bon, J. Massoulié, C. Bon, *FEBS Lett.* **1996**, *387*, 1996 – 2000.
[23] P. N. Alzari, M. B. Lascombe, R. J. Poljak, *Annu. Rev. Immunol.* **1988**, *6*, 555 – 580.
[24] S. Krapp, Y. Mimura, R. Jefferis, R. Huber, P. Sondermann, *J. Mol. Biol.* **2003**, *325*, 979 – 989.
[25] G. L. Ellman, K. D. Courtney, V. Andres, R. M. Featherstone, *Biochem. Pharmacol.* **1961**, *7*, 88 – 90.
[26] P.-A. Ohlsson, T. Tjarnhage, E. Herbai, S. Lofas, G. Puu, *Bioelectrochem. Bioenerg.* **1995**, *38*, 137 – 148.
[27] G. Puu, I. Gustafson, E. Artursson, P.-A. Ohlsson, *Biosens. Bioelectron.* **1995**, *10*, 463 – 476.
[28] A. Tronin, T. Dubrovsky, C. Nicolini, *Langmuir* **1995**, *11*, 385 – 389.

[29] Y. Frobert, C. Créminon, X. Cousin, M.-H. Rémy, J.-M. Chatel, S. Bon, C. Bon, J. Grassi, *Biochim. Biophys. Acta* **1997**, *1339*, 253 – 267.
[30] B. H. J. Hofstee, *Science* **1952**, *116*, 329 – 331.
[31] G. S. Eadie, *J. Biol. Chem.* **1942**, *146*, 85 – 93.
[32] P. R. Coulet, C. Godinot, D. C. Gautheron, *Biochim. Biophys. Acta* **1975**, *391*, 272 – 281.
[33] M. Arrio-Dupont, P. R. Coulet, *Biochem. Biophys. Res. Commun.* **1979**, *89*, 345 – 352.
[34] P. R. Coulet, *J. Membr. Sci.* **1992**, *68*, 217 – 228.
[35] B. Leca, L. J. Blum, *Analyst* **2000**, *125*, 789 – 791.
[36] J. W. Choi, Y. K. Kim, I. H. Lee, J. Min, W. H. Lee, *Biosens. Bioelectron.* **2001**, *16*, 937 – 943.
[37] P. Boullanger, M.-R. Sancho-Camborieux, M.-N. Bouchu, L. Marron-Brignone, R. M. Morélis, P. R. Coulet, *Chem. Phys. Lipids* **1997**, *90*, 63 – 74.
[38] P. Boullanger, J. Banoub, G. Descotes, *Can. J. Chem.* **1987**, *65*, 1343 – 1348.
[39] A. P. Girard-Egrot, R. M. Morélis, P. Boullanger, P. R. Coulet, *Colloids Surf. B* **2000**, *18*, 125 – 135.
[40] A. P. Girard-Egrot, J.-P. Chauvet, P. Boullanger, P. R. Coulet, *Langmuir* **2001**, *17*, 1200 – 1208.
[41] M. Subirade, C. Salesse, D. Marion, M. Pézolet, *Biophys. J.* **1995**, *69*, 974 – 988.
[42] M. Léonard, R. M. Morélis, P. R. Coulet, *Thin Solid Films* **1995**, *260*, 227 – 231.
[43] L. Marron-Brignone, R. M. Morélis, P. R. Coulet, *J. Colloid Interface Sci.* **1997**, *191*, 349 – 356.
[44] R. A. Hann in *Langmuir–Blodgett Films* (Ed.: G. Roberts), Plenum Press, New York, **1990**, p. 17.
[45] L. Marron-Brignone, PhD thesis, Université de Lyon (France), **1997**.
[46] S. F. Altschul, T. L. Madden, A. A. Schaffer, J. Zhang, Z. Zhang, W. Miller, D. J. Lipman, *Nucleic Acids Res.* **1997**, *25*, 3389 – 3402.
[47] P. Gouet, E. Courcelle, D. I. Stuart, F. Metoz, *Bioinformatics* **1999**, *15*, 305 – 308.
[48] H. M. Berman, J. Westbrook, Z. Feng, G. Gilliland, T. N. Bhat, H. Weissig, I. N. Shindyalov, P. E. Bourne, *Nucleic Acids Res.* **2000**, *28*, 235 – 242.
[49] R. Esnouf, *Acta Crystallogr. Sect. D: Biol. Crystallogr.* **1997**, *53*, 665 – 672.
[50] A. T. Brunger, P. D. Adams, G. M. Clore, W. L. DeLano, P. Gros, R. W. Grosse-Kunstleve, J. S. Jiang, J. Kuszewski, M. Nilges, N. S. Pannu, R. J. Read, L. M. Rice, T. Simonson, G. L Warren, *Acta Crystallogr. Sect. D: Biol. Crystallogr.* **1998**, *54*, 905 – 921.
[51] E. A. Padlan, *Mol. Immunol.* **1994**, *31*, 169 – 217.
[52] A. Roussel, C. Cambillau in *Silicon Graphics Geometry Directory* (Ed.: M. View), Silicon Graphics, CA, USA, **1989**, pp. 77 – 78.
[53] B. Leca, R. M. Morélis, P. R. Coulet, *Michrochim. Acta* **1995**, *121*, 147 – 154.

Received: August 2, 2004
Published online: January 13, 2005

